ELSEVIER

Journal of Molecular Catalysis A: Chemical 116 (1997) 421–429

JOURNAL OF MOLECULAR CATALYSIS A: CHEMICAL

Characteristic features of Raman band shifts of vanadium oxide catalysts exchanged with the ^{18}O tracer and active sites for reoxidation

Takehiko Ono *, Hideo Numata

Department of Applied Chemistry, Osaka Prefecture University, 1-1 Gakuen-cho, Sakai, Osaka 593, Japan

Received 27 June 1996; accepted 18 October 1996

Abstract

The oxide oxygen ions of V_2O_5 catalyst were exchanged with ^{18}O tracer by a reduction–oxidation method and by a catalytic oxidation of *n*-butane using $^{18}O_2$. The Raman band shifts of the V_2O_5 exchanged with ^{18}O by the methods were examined. The band at 700 cm^{-1} was shifted to lower frequencies more preferentially than the band of V=O oxygen at 998 cm^{-1}. Applying the correlation between the Raman bands and stretching modes as described in the literature, the positions of oxide ions and anion vacancies for reduction and reoxidation were estimated. The anion vacancies corresponding to the V–O species in the V square with 1.88 and 2.02 Å distances seem to be active sites for oxygen insertion. The similar conclusions were obtained for Mo containing V_2O_5 catalyst.

Keywords: Vanadium oxide; Raman spectroscopy; Tracer technique

1. Introduction

Previously, we have investigated the Raman band shifts of Bi–Mo oxides [1,2], β-$CoMoO_4$ [2], α-$MnMoO_4$ [2], and MoO_3 [3] by the exchange ^{18}O tracer through oxidation reactions. With MoO_3 [3] and α-$Bi_2Mo_3O_{12}$ [2] catalysts, it was informed that the oxygen insertion seems to take place selectively at the oxygen vacancies corresponding to the Mo–O–Mo oxygen ions rather than Mo=O oxygen. On the other hand, with α-$MnMoO_4$ [2] catalyst, it was elucidated that the oxygen vacancies corresponding to the shortest Mo=O are responsible for reoxidation at initial stages. With β-$CoMoO_4$ catalyst [2], the different features were observed. In the oxidation reactions on V_2O_5 catalysts, it has been established that the redox mechanism takes place on the catalysts [4–8]. Some workers have proposed that the V=O oxygen is responsible for oxidation reactions over V_2O_5 catalysts [9,10] while it has been recently reported that the V–O–V oxygen is responsible for them over V_2O_5/Al_2O_3 catalyst [11]. Using ^{18}O tracer, the oxygen species on V_2O_5 responsible for oxidation was also studied in the past [12–14].

In this work, the oxide ions of V_2O_5 and Mo containing V_2O_5 catalyst were exchanged with

* Corresponding author. Fax: +81-722-593340; e-mail: ono@chem.osakafu-u.ac.jp.

PII S1381-1169(96)00425-6

^{18}O tracer via *n*-butane oxidation. The Raman spectra of partly exchanged V_2O_5 with ^{18}O were measured and the preferential shifts of the bands were compared. The correlation between the Raman bands and the stretching normal modes reported previously on V_2O_5 [15,16] was applied to the estimation of oxygen species and anion vacancies. Then, the nature of redox sites on V_2O_5 and Mo containing V_2O_5 were discussed.

2. Experimental

2.1. Preparation of catalysts

The V_2O_5 and Mo containing V_2O_5 catalysts supported on SiO_2 (10 wt%) was prepared as follows: the desired amounts of ammonium metavanadate were mixed with SiO_2 in the NH_3 solution. After evaporation on a water bath, it was heated at 723 K for 6 h. The desired amount of ammonium metavanadate and ammonium heptamolybdate were mixed with SiO_2 in the NH_3 solution. The 5, 10, and 15 at% of Mo in the V_2O_5 catalysts were prepared. After evaporation, they were also heated at 723 K for 6 h.

2.2. Procedures for O exchange

The exchange of the lattice oxygen of the catalysts with ^{18}O were performed by two methods. The first method, a reduction–oxidation method, is as follows: the reduction of catalysts by *n*-butane was carried out in a circulation system (ca. 360 cm^3) at ca. 4 kPa and 700–750 K and the reoxidation by $^{18}O_2$ (98.1 at%, Isotec) was carried out at the same temperature. The second method for exchange is as follows: the mixture of *n*-butane at ca. 4 kPa and $^{18}O_2$ at ca. 1 kPa was reacted on V_2O_5/SiO_2 catalysts. The reaction products were butenes, buta-1,3-diene, CO, and CO_2, whose ^{18}O percents were determined using a mass spectrometer (Shimadzu GCMS QP2000A). The amounts of ^{18}O exchanged in the V_2O_5 catalyst were assumed as those of ^{16}O in the products.

The structure of catalysts was determined by an X-ray diffraction method using CuKα radiation. The laser Raman spectra of the catalyst samples exchanged with ^{18}O were recorded on a JASCO NR-1000 laser Raman spectrometer. An Ar-ion laser was tuned to 514.5 nm for excitation. The laser power was set at 150–200 mW. The data were stored on a computer and the peak-shape analysis was carried out using the technique reported by Miyata et al. [17,18].

3. Results and discussion

3.1. Structure of V_2O_5, Raman spectra of V_2O_5, and assignments to the normal vibrations

The structure of V_2O_5 was investigated by some workers in the past [19,20]. It is described as a layer structure which is built up by VO_6 distorted octahedra as shown in Fig. 1. These octahedra are linked by edge-sharing and corner-sharing. Fig. 2a shows the Raman spectra of V_2O_5. The bands at 998, 703, 530, 485, 410, 304, and 293 cm^{-1} are found.

Abello et al. [15] have reported the Raman and IR spectra of V_2O_5 crystal on the basis of normal co-ordination analysis using $(V_2O_4)_n$,

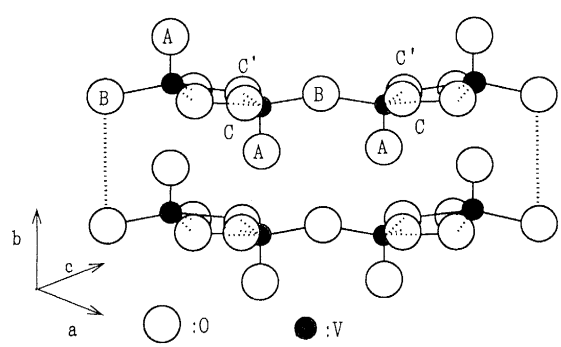

Fig. 1. Structure of V_2O_5 [19,20]. The related V–O distances are as follows: V–O_A: 1.58 Å, V–O_B: 1.77 Å, V–O_C: 1.88 Å. The O_A corresponds to oxygen of OV, O_B to OV_2, and O_C to OV_3 in the Beattie's model [16].

Table 1
Normal stretching modes of V_2O_5 crystal and Raman spectra assigned by Abello et al. [15] and Beattie et al. [16]

Abello's $(V_2O_5)_n$ model (mode, band (cm^{-1}))	Beattie's model (mode, band (cm^{-1}))	Related V–O distance (Å)	Raman bands in this work
A_g (V–O_A) 994	a_g, b_{1g} (OV) 996	1.58 Å	998
A_g (V–O_B–V) 526	a_g (OV_3) 530	1.77(2) [a]	530
B_{2g} (V–O_C) 700	b_{2g}, b_{3g} (OV_3) 703	1.88(2)	703
		2.02	

[a] In the case of Abello's model. The numerals in ( ) denote the number of bonds.

$(V_2O_5)_n$, and special V_2O_7 models. As shown in Fig. 1 and Table 1, the V_2O_5 unit consisted of two O_C (or $O_{C'}$), two O_A, one O_B and two V ions. According to this model, the band at 998 cm^{-1} corresponds to the V–O_A vibration at 1.58 Å, i.e., terminal oxygen. The band at 700 cm^{-1} corresponds to the V–O_C vibration at 1.88 Å. The band at 530 cm^{-1} corresponds to V–O_B–V vibration where the dominant displacement takes place on V atoms. Beattie and Gilson [16] studied the vibrational spectra of V_2O_5 applying group frequency assignments. According to their work, the bands at 994 cm^{-1} corresponds to OV, that at 703 cm^{-1} to OV_3 (high), that at 530 cm^{-1} to the OV_3 (low) vibrations, respectively. The assignments of the 998 and 703 cm^{-1} bands are classified to the similar stretching vibrations between the Abello's and Beattie's models. But those at 530 cm^{-1} are different.

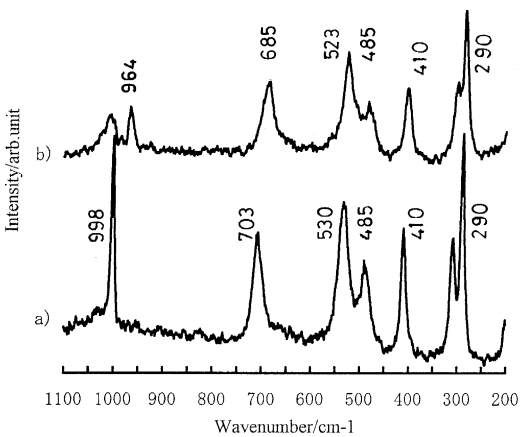

Fig. 2. (a) Original Raman spectra of V_2O_5/SiO_2 (*10 wt% of V_2O_5*), (b) spectra of V_2O_5/SiO_2 exchanged with $^{18}O_2$ at 873 K for more than 24 h.

3.2. The determination of Raman band shifts of V_2O_5 exchanged with ^{18}O

The oxygen ions of V_2O_5 were exchanged sufficiently using $^{18}O_2$ at 873 K for more than 24 h in order to get the final position of the bands of V_2O_5. Fig. 2 also shows the Raman spectra of V_2O_5 unexchanged and exchanged with ^{18}O. The bands at 998 and 703 cm^{-1} shift to 964 and 685 cm^{-1}, respectively. The band at 530 cm^{-1} shifts to 523 cm^{-1}, whose interval is very small. The other bands below 480 cm^{-1} show little or no shift, which belong to the bending vibrations.

Table 2 shows the shift intervals in the case of theoretical calculation for V–^{18}O stretching vibrations. The shift interval of the 998 cm^{-1} band is 34 cm^{-1}, which is ca. 80% of the calculated one. It may be applicable to diatomic vibration. With the 700 cm^{-1} band, the experimental interval (18 cm^{-1}) is smaller than the calculated one (30 cm^{-1}). This should cause to the deviation from the V–O_C diatomic stretching model. A very small shift with the 530 cm^{-1} band will cause to the fact that the domi-

Table 2
Raman band shift of V_2O_5 catalyst exchanged with ^{18}O and calculated values [a] by diatomic approximation

Observed spectra (cm^{-1})			Calculated difference (m^{-1})
original	after exchange	difference	
998	964	−34	−43
703	685	−18	−30
530	523	−7	−23

[a] Calculated from (original band $cm^{-1} \times (\mu(V, {}^{16}O)/\mu(V, {}^{18}O))^{1/2}$, where μ is reduced mass.

Table 3
n-Butane conversion, product selectivity, and average ^{18}O exchange percentage over V_2O_5/SiO_2 catalyst

Temp. (K)	Conv. (%)	Selectivity (%)		Average exchange (^{18}O% in V_2O_5)
		$C_4H_6+C_4H_8$	$CO+CO_2$	
710 [a]	0.36	65	35	4
731 [a]	0.73	73	27	6
748 [a]	1.3	80	20	10
788 [a]	1.5	88	12	17
717 [b]	0.73	14	86 (27, 19) [c]	8
728 [b]	2.2	13	87 (34, 27) [c]	27

[a] The catalyst was reduced by *n*-butane at ca. 3 kPa and reoxidized by $^{18}O_2$ at ca. 1 kPa over 0.05 g of catalyst for 5 min.
[b] The catalyst oxygen was exchanged by the catalytic oxidation at ca. 3 kPa of *n*-butane and ca. 1 kPa of $^{18}O_2$ over 0.05 g of catalysts for 5 min.
[c] The numerals in ( ) denote the ^{18}O% in CO and CO_2, respectively. The ^{18}O% in H_2O were estimated from those in CO and CO_2.

nant vibrating atom is the vanadium cation, which is suggested by Abello's model [16].

3.3. Raman band shifts of V_2O_5 catalyst exchanged with ^{18}O by a reduction–oxidation method

0.05 g of V_2O_5/SiO_2 (10 wt%) was reduced with *n*-butane at 710–750 K. After evacuation, it was reoxidized with $^{18}O_2$ at the same temperature. The product selectivities in the reduction by *n*-butane were shown in the Table 3. The selectivity to butenes + buta-1,3-diene ranges ca. 65 to 80%. The average exchange ^{18}O% are also listed in Table 3, which were calculated from the amounts of ^{16}O in the products, assuming that the reoxidation of V_2O_5 takes place completely. Fig. 3 shows the spectra of V_2O_5 before and after they were exchanged with ^{18}O. At low exchange %, the band at 700 cm^{-1} shifts to low frequencies and shows line broadening. At high exchange %, the new band at 964 cm^{-1} appears, which is shifted from 998 cm^{-1}. The 700 cm^{-1} band shifts to 685 cm^{-1} finally.

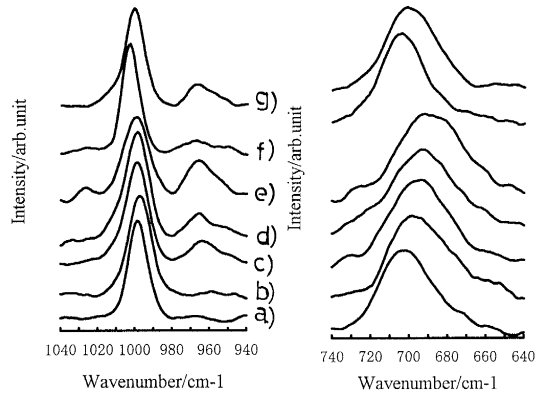

Fig. 3. Raman spectra of V_2O_5/SiO_2 (*10 wt% of* V_2O_5) exchanged with ^{18}O tracer using a reduction–oxidation method. (a) No change, (b) 4% of ^{18}O exchanged (c) 6%, (d) 10%, (e) 17%. Those by using a catalytic oxidation (f) 8% and (g) 27%. See also Table 3.

In order to know the shift change in details, the peak shape analysis was attempted with these spectra using Gaussian function [17,18] (Fig. 4). The broad band at ca. 700 cm^{-1} was separated to 703 and 685 cm^{-1} bands since the latter band was determined experimentally. Table 4 shows the shifted fractions for the 998

Table 4
Fractions obtained from band-shape analysis for the 703 and 998 cm^{-1} bands for V_2O_5 catalyst

Reaction temp. (K)	Average exchanged (% in V_2O_5)	Exchange % at 703 cm^{-1} $I_{685}/(I_{703}+I_{685})$	Exchange % at 998 cm^{-1} $I_{998}/(I_{998}+I_{965})$
710 [a]	4	27	9
731 [a]	6	27	16
748 [a]	10	46	20
788 [a]	17	56	29
717 [b]	8	22	11
728 [b]	27	40	18

[a] and [b] express the same meanings as in Table 3.

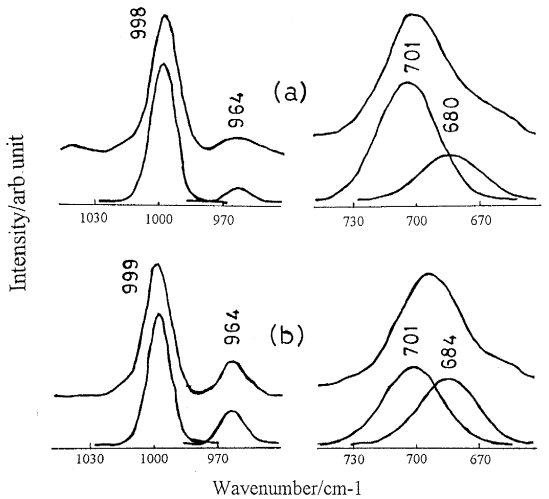

Fig. 4. The peak shape analysis of (a) spectra of Fig. 3b, and (b) those of Fig. 3d.

cm^{-1} and 703 bands. With the 4% sample, the fractions of 998 and 700 cm^{-1} bands are 9% and 27%, respectively. The latter is ca. 3 times higher than the former. With the higher percent samples, the fractions of the 700 cm^{-1} band are always higher than those of the 998 cm^{-1} band. These results suggest that oxygen insertion from gas phase takes place at the vacancies corresponding to the 1.88 Å position (O_C) in the V square rather than at the 1.58 Å position (O_A) in the oxygen layer.

The exchange fractions with 998 and 700 cm^{-1} bands are extremely higher than the average exchange % (Table 4). This suggests that the information of Raman spectra comes from the near surface of V_2O_5 crystal and that the surface oxygens are well reacted and exchanged. Similar results were obtained for MoO_3 [3] and Bi–Mo oxide [2] catalysts.

3.4. Raman band shifts of V_2O_5 catalyst exchanged with ^{18}O by a catalytic oxidation using n-butane and $^{18}O_2$

The catalyst oxygen ions were exchanged with ^{18}O via catalytic oxidation using *n*-butane and $^{18}O_2$ over the V_2O_5 (15 wt%)/SiO_2 catalyst. The conversion, product selectivity, and average ^{18}O% in the products are also shown in Table 3. The average ^{18}O% of the catalysts were calculated from the ^{16}O% of products such as CO, CO_2, and H_2O. Fig. 5 and Table 4 show the Raman spectra and the results of peak-shape analysis. The fractions of the 700 cm^{-1} band are ca. 2 times bigger than those of the 998 cm^{-1} bands. This tendency is the same as that in a reduction–oxidation method. The results indicate that the oxygen insertion in the catalytic oxidation takes place preferentially at the position V–O_C vacancies (V–O layer) rather than the position V–O_A (oxygen layer).

3.5. Active sites for reoxidation on V_2O_5

As discussed above, the band at 700 cm^{-1} is corresponding to the stretching vibration of V–O_C with 1.88 Å (2.02 Å) in the V square of octahedron. These are also edge-linked oxygen ions between two octahedra. The band at 998 cm^{-1} corresponds to the terminal V=O of 1.58 Å, which is called oxygen layer. The results indicate that the V square oxygen ions are replaced more preferentially than those of the oxygen layer. It is concluded that the oxygen insertion takes place at the vacancies corre-

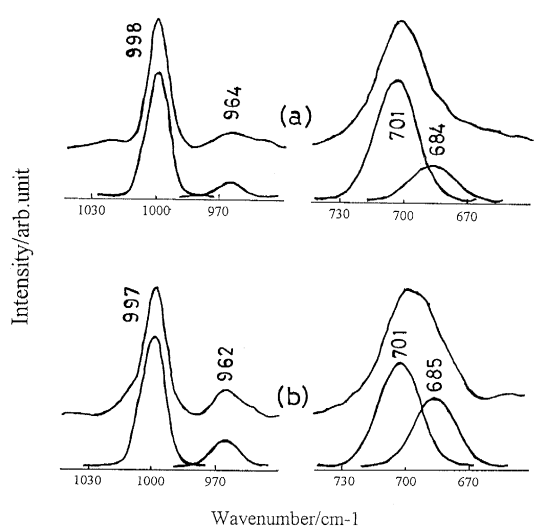

Fig. 5. The peak shape analysis of (a) spectra of Fig. 3f, and (b) those of Fig. 3g.

sponding to $V-O_{C_o}$ oxygen. The oxygen of $V-O_B$ for 1.77 Å, which corresponds to corner-linked oxygen between two octahedra, will also be replaced, though the information from the Raman band could not be obtained in this work. These features of V_2O_5 are similar to those of MoO_3 [3]. The two bands at 823 and 670 cm^{-1} of MoO_3 were shifted to lower frequencies preferentially while the bands of terminal Mo=O oxygen at 998 cm^{-1} were not shifted very much initially. This indicated the anion vacancies of Mo square seem to be active sites for oxygen insertion [3].

The study of reduction of V_2O_5 was performed by some workers. Kawashima et al. [21], reported the existence of intermediate phases from V_2O_5 by reduction with SO_2. These phases were expressed V_NO_{2N+1} which were produced by the loss of oxygen layers, i.e., terminal oxygen ions. Colpaert et al. [22], reported the presence of shear planes at the boundary between V_2O_5 and V_6O_{13} where the rate of oxygen loss was enhanced. From these results, it has been proposed that the oxygen layer, i.e., V=O oxygen, is responsible for the reduction by such as SO_2 and hydrocarbons. However, it seems to be unclear which oxygen is responsible at the initial step. The loss of oxygen layer may occur via high migration of oxygen after the reaction takes place at the V square.

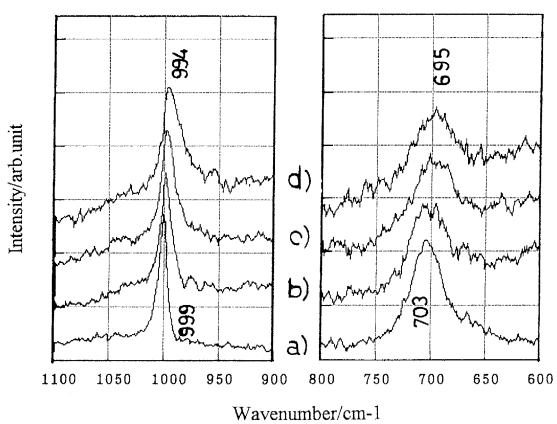

Fig. 6. Raman spectra of Mo containing V_2O_5 catalysts as a function of Mo content. (a) V_2O_5, (b) 5 at% of Mo, (c) 10%, and (d) 15%.

If the anion vacancies move easily to other sites after the reduction on V_2O_5, reoxidation may occur randomly at various vacancies, i.e., ^{18}O exchange will occur equally at various oxygen ions. The paired oxygen insertion mechanisms were previously proposed by Novakova [27] and Hirota et al. [12]. In this work, the preferential exchange takes place on the V square of octahedra rather than terminal oxygen. The insertion of the two oxygen atoms seems to occur at the vacancies of the V square according to that assumption [12,27].

3.6. Raman spectra of Mo containing V_2O_5 catalysts and their shift intervals with ^{18}O exchange

Fig. 6 shows Raman spectra of Mo containing V_2O_5 catalyst before using for reactions. The bands at 998 and 700 cm^{-1} shift slightly to lower frequencies with the increase in Mo content. With the 15 Mo at% catalyst, the bands at 999 and 703 cm^{-1} shift to 994 and 695 cm^{-1}, respectively. In this work, it is confirmed that both V–O bonds at 998 and 703 cm^{-1} are weakened due to the presence of Mo ions. According to previous reports [9], the formation of solid solution of Mo ions to V_2O_5 bring about O_2 evolution and V^{4+} formation during heating. The decrease in the V=O band at 998 cm^{-1} should be caused by such replacement with Mo ions [9]. ESR studies revealed that the electron of a V^{4+} ion interacted with several neighbor V^{5+} ions in the V_2O_5 crystal [23].

The Mo 5 at% V_2O_5 catalyst was exchanged with ^{18}O sufficiently for a long exchange time at 873 K (Fig. 7) to know the final shift positions. At the middle exchange time as shown in Fig. 7b, the band at 998 cm^{-1} shifts to 965 cm^{-1}. The band at 700 cm^{-1} shows line broadening. These shift positions seem to be nearly the same as those with V_2O_5 shown in Table 2. With the sample which was exchanged to final extent as shown in Fig. 7c, both bands at 998

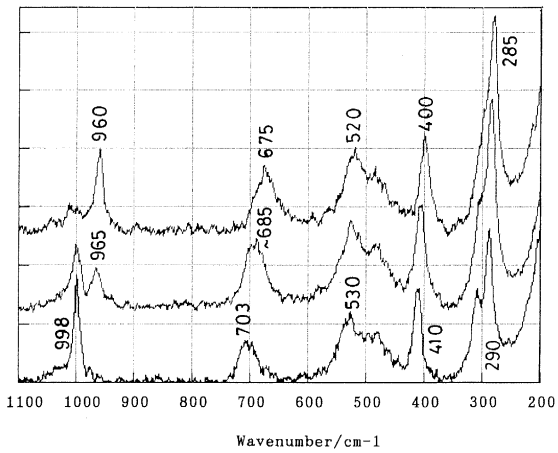

Fig. 7. Raman spectra of Mo containing (5 at%) catalyst exchanged with ^{18}O sufficiently. (a) no exchange. (b) Exchanged with $^{18}O_2$ at 0.5 kPa and 823 K for 40 h after reduction by *n*-butane for 10 min. (c) The cycle of (b) was repeated 4 times except $^{18}O_2$ exposure time was 10 h each.

and 700 cm^{-1} shift to lower frequencies such as 960 and 675 cm^{-1}, respectively. These values are somewhat smaller than those with V_2O_5. This latter feature seems to accompany the Mo enrichment at the V_2O_5 surface by repeating reduction and reoxidation for many times. The Mo enrichment should be evidenced by XPS.

3.7. Raman band shifts of Mo containing V_2O_5 catalyst exchanged with ^{18}O by a reduction–oxidation method

0.05 g of MoO_3–V_2O_5/SiO_2 (Mo 5 at%) was reduced with *n*-butane at 673–773 K. After evacuation, it was reoxidized with $^{18}O_2$ at the same temperature. The product selectivities in the reduction by *n*-butane were shown in Table 5. The selectivity to butenes + buta-1,3-diene ranges from ca. 35 to 40% which are somewhat smaller than in the case of V_2O_5. The average exchange ^{18}O% were calculated from the amounts of ^{16}O in the products. Fig. 8 shows the spectra as a function of the percentage exchanged with ^{18}O. At low exchange percentage, no shift is observed at the band at 999 cm^{-1} but the band at 703 cm^{-1} shifts to low frequencies and shows line broadening. At high exchange

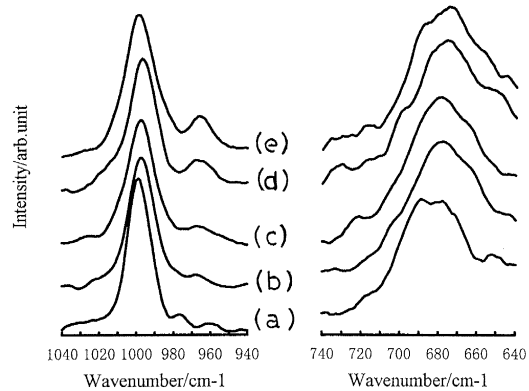

Fig. 8. Raman spectra of Mo containing (5 at%) V_2O_5/SiO_2 exchanged with ^{18}O tracer using a reduction–oxidation method. (a) No change, (b) 5% of ^{18}O exchanged (c) 11%, (d) 12%, and (e) 33%.

percentage, the new band at 965 cm^{-1} appears, which is shifted from 998 cm^{-1}.

In order to elucidate the shift change, the peak shape analysis was attempted using the shift position 964 and 685 cm^{-1} because the shift intervals were the same as those with V_2O_5 at a short exchange time as described above. Fig. 9 shows the examples of peak shape analysis of Fig. 8. Table 6 lists the band intensity fractions. With the 5–11% of average exchange, the shift fractions at 998 cm^{-1} are small and the

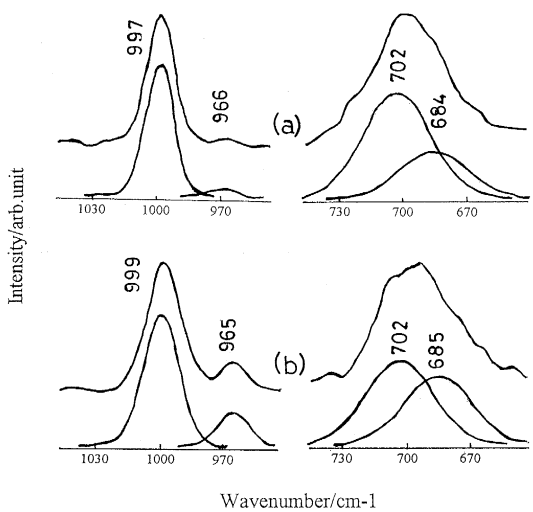

Fig. 9. The peak shape analysis of (a) spectra of Fig. 8b, and (b) that of Fig. 8e.

Table 5
n-Butane conversion, product selectivity, and average ^{18}O exchange percentage over Mo containing (5 at%) V_2O_5/SiO_2 catalyst

Temp. (K)	Conv. (%)	Selectivity (%)		Average exchange (^{18}O% in MoO_3/V_2O_5)
		$C_4H_6 + C_4H_8$	$CO + CO_2$	
703	0.4	30	70	5
716	0.7	29	71	11
733	1.0	45	55	12
753	2.1	32	68	33

The catalyst was reduced by *n*-butane at ca. 3 kPa for 5 min and reoxidized by $^{18}O_2$ at ca. 1 kPa over 0.05 g of catalyst.

fractions at the 700 cm^{-1} band are 6–3 times larger than those at the 998 cm^{-1} band. These results indicate that catalyst reoxidation takes place preferentially at the 700 cm^{-1} band corresponding to the 1.88 and 2.02 Å, i.e., $V–O_C$. The tendency is the same as that with V_2O_5. Previously, the propene oxidation over MoO_3/V_2O_5 catalysts was studied [14]. Our previous work indicated that the Mo containing catalyst had higher activity and that the lattice oxygen participation by using ^{18}O tracer became higher because of V^{4+} formation and that it lead to the increase of anion vacancies and of lattice oxygen mobility. The difference between the exchanged fraction of $V–O_C$ oxygen and terminal $V=O_A$ oxygen is somewhat bigger for Mo containing V_2O_5 catalysts. This suggests that the more rapid diffusion in the bulk due to the presence of Mo ions slightly affects the preferential exchange of O_C oxygen in the V square.

3.8. Redox features on V_2O_5 and Mo containing V_2O_5 catalysts

As has been proposed by a number of workers (e.g. Ref. [24]), the reduction of the oxides and its oxidation by gaseous oxygen occurs in different regions on the oxide catalysts such as Bi–Mo oxides. The surface anion vacancies formed in the region X are refilled by diffusion of oxide ions in the bulk, which results in formation of the surface anion vacancies in the region C. These vacancies bring about the oxygen insertion. Under such situation, the following equation holds under the steady state of oxygen flow [14,25,26]. It is a modified redox mechanism instead of a Mars and van Krevelen mechanism [4]:

$$k_1 P_{C4H8} \Theta_X = k_2 P_{O2}^{1/2} (1 - \Theta_C)$$

where Θ_X and $1 - \Theta_C$ refer to the surface fractions of oxide ions and vacancies in the region X and C, respectively. k_1 is the rate

Table 6
Fractions obtained from band shape analysis for the 703 and 998 cm^{-1} bands for Mo containing (5 at%) V_2O_5 catalyst

Reaction temp. (K)	Average exchanged (% in V_2O_5)	Exchange % at 703 cm^{-1} $I_{685}/(I_{703} + I_{685})$	Exchange % at 998 cm^{-1} $I_{965}/(I_{998} + I_{965})$
703	5	30	5
716	11	28	9
733	12	39	16
753	33	45	19

constant for the reduction step and k_2 for the reoxidation step. With V_2O_5 and Mo containing V_2O_5 in this work, similar situations will be expected. From our results it is elucidated that the reoxidation occurs at the vacancies corresponding to O_C in the V square, i.e., the C region corresponds to the O_C oxygen ions here. It is unclear which oxygen (O_X) will react with *n*-butane at the initial reduction step. Tarama et al. [9] reported that the O_A in Fig. 1, i.e., V=O oxygen, is responsible for the reaction and that the promotive action of MoO_3 is due to the weakening of the V=O bond by its solid solution. In this work, the bond weakening takes place at other V–O bonds as well as V=O bonds. If the V=O_A oxygen reacts preferentially as proposed previously, the reoxidation and exchange seems to take place at the V=O position more preferentially. However, such a feature was not observed. The O_X may be also O_C or O_B species which are somewhat far apart from each other in the edge- and corner-linked V squares.

Acknowledgements

We thank Professor Hisashi Miyata for help in computer peak shape analysis. We also thank Professor Masakazu Anpo for using the Shimadzu Mass Spectrometer(GCMS QP2000A).

References

[1] T. Ono and N. Ogata, J. Chem. Soc. Faraday Trans. 90 (1994) 2113.
[2] T. Ono, N. Ogata and Y. Miyaryo, J. Catal. 160 (1996) in press.
[3] T. Ono, H. Numata and N. Ogata, J. Mol. Catal. A: Chemical 105 (1996) 31.
[4] P. Mars and D.W. van Krevelen, Chem. Eng. Sci. Suppl. 3 (1954) 41.
[5] J.M. Weiss and G.R. Hill, J. Phys. Chem. 59 (1955) 388.
[6] G.l. Simard, J.F. Steger, R.J. Arnott and L.A. Siegel, Ind. Eng. Chem. 47 (1955) 1424.
[7] T. Matsuura, Nippon Kagakukai-shi 82 (1961) 276, 417.
[8] T. Seiyama and N. Takeyama, Metallugie 7 (1967) 161.
[9] K. Tarama, S. Teratani, S. Yoshida and N. Tamura, Proc. 3rd Int. Congr. on Catalysis, Amsterdam (1964) p. 287.
[10] M. Inomata, A. Miyamoto and Y. Murakami, J. Catal. 62 (1980) 140.
[11] J.G. Eon, R. Olier and J.C. Volta, J. Catal. 145 (1994) 318.
[12] K. Hirota, Y. Kera and Teranishi, J. Phys. Chem. 72 (1968) 3133; Y. Kera and K. Hirota, J. Phys. Chem. 78 (1969) 3973; Y. Kera, Bull. Chem. Soc. Jpn. 50 (1977) 2841.
[13] A. Miyamoto, K. Mori, M. Miura and Y. Murakami, Ads. Catal., Oxid. Surface (Elsevier, 1985) p. 371.
[14] T. Ono and Y. Kubokawa, Bull. Chem. Soc. Jpn. 55 (1982) 1748.
[15] L. Abello, E. Husson, Y. Repelin and G. Lucazeau, Spectrochim. Acta 39A (1983) 641.
[16] I.R. Beattie and T.R. Gilson, J. Chem. Soc. A (1969) 2322.
[17] H. Miyata, K. Fujii, S. Inui and Y. Kubokawa, Appl. Spectrosc. 40 (1986) 1177.
[18] H. Miyata, S. Tokuda and T. Yoshida, Appl. Spectrosc. 43 (1989) 522.
[19] A. Bystrom, K.A. Wilhelmi and O. Brozen, Acta Chem. Scand. 4 (1950) 1119.
[20] H.G. Bachmann, F.R. Ahmed and W.H. Barnes, K. Krist. 115 (1961) 110.
[21] K. Kawashima, K. Kosuge and S. Kachi, Chem. Lett. (1975) 1131.
[22] N.L. Colpaert, P. Clauws, L. Fiermans and J. Vennik, Surf. Sci. 36 (1973) 513.
[23] K. Hirota, K. Kuwata and Y. Kera, Bull. Chem. Soc. Jpn. 43 (1970) 3617.
[24] T.D. Snyder and G.C., Hill Jr., Catal. Rev. Sci. Eng. 31 (1989) 43.
[25] T. Ono, T. Nakajyo and T. Hironaka, J. Chem. Soc. Faraday Trans. 86 (1990) 4077.
[26] T. Ono, M. Kiryu, M. Komiyama and R.L. Kuczkowski, J. Catal. 127 (1991) 618.
[27] J. Novakova, Catal. Rev. 4 (1971) 77.